Sensitivity of input parameters to modelling of atmospheric transmission of long-wave infrared radiation at sea under warm and humid conditions

Jan Thomassen, Arthur D. van Rheenen, Eirik Blix Madsen, Mark Pszczel, Nicola Bilton, et al.

Jan Thomassen, Arthur D. van Rheenen, Eirik Blix Madsen, Mark Pszczel, Nicola Bilton, Oleksandr Pushkarov, "Sensitivity of input parameters to modelling of atmospheric transmission of long-wave infrared radiation at sea under warm and humid conditions," Proc. SPIE 10794, Target and Background Signatures IV, 107940A (9 October 2018); doi: 10.1117/12.2324976

SPIE.

Event: SPIE Security + Defence, 2018, Berlin, Germany

Sensitivity of input parameters to modelling of atmospheric transmission of long-wave infrared radiation at sea under warm and humid conditions

Jan Thomassen[a], Arthur D van Rheenen[a], Eirik Blix Madsen[a], Mark Pszczel[b], Nicola Bilton[b], and Oleksandr Pushkarov[b]

[a]Norwegian Defence Research Establishment (FFI), PO Box 25, N-2027 Kjeller, Norway
[b]Defence Science and Technology Group, PO Box 1500, Edinburgh SA 5111, Australia

ABSTRACT

A joint Australian-Norwegian field trial (Osprey) was held in February 2018 in Darwin, Australia. The objective of this trial was to measure IR transmission properties of the atmosphere in a marine environment under warm and humid conditions. Darwin is in the tropics (longitude 12° south), and February is the middle of the "wet season". Various temperature-controlled sources (blackbodies) were used during the trial. Land based weather stations recorded a number of meteorological data. The sensors used in the trial included long-wave, mid-wave and short-wave IR cameras. In this paper we present the analysis of measurements performed on two blackbodies across Darwin Harbour. The scene was recorded with an IRCAM LW camera and calibrated to blackbodies with known temperature. We have modelled the atmospheric transmittance using MODTRAN, and from this acquired the equivalent blackbody temperature of the scene. In our analysis, we are not only interested in the overall agreement between predictions and data, but also on the sensitivity of the predictions to uncertainties of the input parameters (calibration temperatures, air temperature, humidity, etc.). In order to study this sensitivity, we used variance based sensitivity analysis and Monte Carlo simulations to compute sensitivity indices, according to methods developed by Saltelli and others. Our main finding is that uncertainties in calibration parameters (blackbody and camera temperatures) give the dominant contributions to the error in the computed equivalent temperature.

Keywords: Sensitivity analysis, atmospheric transmission, infrared, signature analysis, Monte Carlo simulations

1. INTRODUCTION

One ingredient in infrared (IR) signature analysis of ships at sea is the calculation of equivalent blackbody temperatures. The computation involves the recording of cold and hot calibration blackbodies in addition to the recording of the scene with the target. We then use MODTRAN[1] to find the atmospheric transmittance. Finally, the equivalent blackbody temperature T_{eq} is found by inverting a function involving a spectral radiance integral. The inputs to this calculation include the temperature and emissivity of the calibration blackbodies and meteorological parameters for running MODTRAN.

What are the errors in the output from this model as a result of input errors? The complexity of the model makes it impossible to compute this analytically, for instance by the method of propagation of errors. In particular, contributions from atmospheric transmittance is difficult because MODTRAN is a computer program and a black box from the point of view of the user. Fortunately, other methods that answer these kinds of questions exist, based on Monte Carlo simulations. A method of variance based sensitivity analysis has been developed in recent years by Saltelli and others.[2,3] This method produces two numbers for each input parameter X_i, the first order sensitivity index S_i and the total-effect index S_{Ti}. These indices describe the effects that variations in the input parameters have on the variance of the model output, as will be described later.

Further author information: (Send correspondence to J.T.)
J.T.: E-mail: jbt@ffi.no, Telephone: +47 63 80 79 21

Target and Background Signatures IV, edited by Karin U. Stein, Ric Schleijpen,
Proc. of SPIE Vol. 10794, 107940A · © 2018 SPIE · CCC code:
0277-786X/18/$18 · doi: 10.1117/12.2324976

In this paper we perform sensitivity analysis on the model for equivalent blackbody temperature. The inputs to this model are 10 parameters, related to the calibration procedure, and the MODTRAN calculations. These inputs were collected during the joint Australian-Norwegian field trial Osprey, held in February 2018 in Darwin, Australia. The environment is such that the contributions from the atmosphere are considerable. It is therefore an interesting case for sensitivity analysis. The model predicts a T_{eq} slightly lower than the measured value. However, our main finding is that the dominant contributions to the variance in the model output comes from three calibration parameters: blackbody temperatures and air temperature.

2. MEASUREMENT SETUP

The joint Australian-Norwegian field trial Osprey was held in February 2018 in Darwin, Australia. The objective of this trial was to measure IR transmission properties of the atmosphere in a marine environment under warm and humid conditions. Darwin is in the tropics (longitude 12° south), and February is the middle of the "wet season". Two ships were used during the trial, instrumented with GPS, temperature sensors (iButtons) and temperature-controlled hot sources (blackbodies). In addition, two pairs of blackbodies were mounted on land: One pair across the Darwin harbour at 3.4 km distance from the measurement site (to measure propagation over sea), and one pair at 140 m distance (to measure the effects of heavy rain showers). Both measurement-teams had land-based weather stations recording meteorological data. Sensors used in the trial included long-wave (LW), mid-wave (MW) and short-wave (SW) IR cameras.

2.1 Location

Measurements were performed from a pier at East Arm Wharf, which is a facility at Darwin Port. (GPS coordinates: 12°29′12.2″S, 130°52′35.6″E.) The two ships that were used during the trial performed a number of runs sailing in different patterns in the east-west direction – outbound from and inbound towards East Arm Wharf. The targets of interest in this paper were the two blackbodies mounted at Stokes Hill Wharf, at a distance of 3.4 km from the measurement site. (GPS coordinates: 12°28′11.9″S, 130°51′01.8″E.) The distances can be found from Google Maps, and the uncertainty of this distance measurement is estimated to be less than 10 m. See Fig. 1 for a map over the geography.

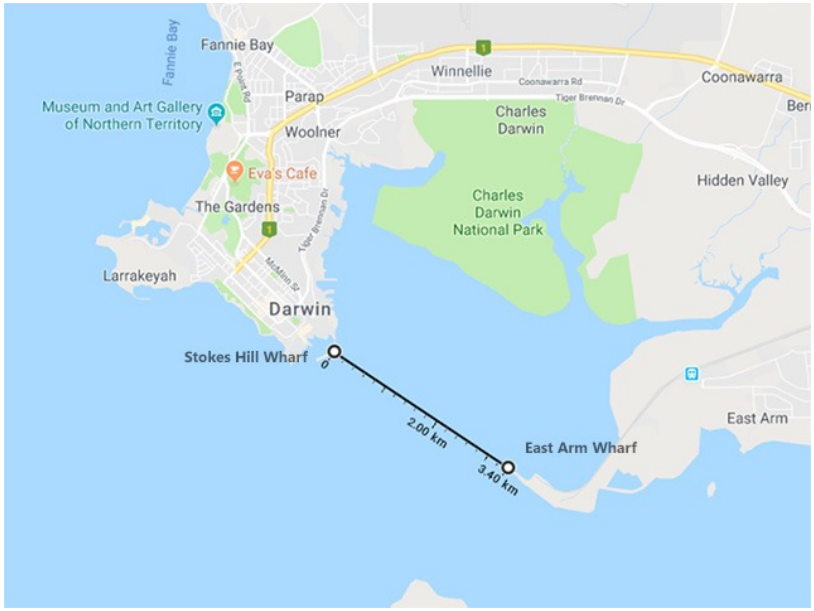

Figure 1. Darwin harbour area. The distance from the measurement site at East Arm Wharf to the blackbodies at Stokes Hill Wharf was approximately 3.4 km. GPS coordinates (12°29′12.2″S, 130°52′35.6″E) and (12°28′11.9″S, 130°51′01.8″E), respectively. Map data ©2018 Google.

2.2 Targets

For the analysis in this paper, one set of measurements of the land based blackbodies at Stokes Hill Wharf were chosen. There were several reasons for this:

- *Complexity*: The complexity of the analysis is high. Using other types of measurements, like recordings of an inbound or outbound ship at various distances would only add to this complexity, without gaining any more insight.
- *Problems with equipment*: The FFI measurement team suffered a camera malfunction early in the trial (the IRCAM MW camera broke down). Also, for the recordings of the ships, the other sensors were used in a new and unusual configuration, which unfortunately led to saturation of the detector signal (LW camera).
- *Data quality*: The recordings of the blackbodies at Stokes Hill Wharf were not affected by the above mentioned problems, and since temperatures, distance measurements and meteorology were under control, it was determined that the quality of these data were satisfactory and suitable for the analysis.

The blackbodies were two water vessels, 1 x 1 m square, 12 cm deep. They were mounted side-by-side on the pier, see Fig. 2. Heating elements kept the two blackbodies at different temperatures, which was measured by two surface mounted PT100 temperature sensors. A provisional "sun screen" was built up around them to keep them out of direct sunlight.

The surface of the blackbodies had been painted with high emissivity "blackbody paint" – Nextel Velvet Coating 811-21. The emissivity of this paint has been measured in a laboratory to be 0.975 ± 0.004 in the temperature ranges we operated.[4] However, the true emissivity of the targets is probably lower, due to "wear and tear of the paint and a thin layer of sea spray that coated the surface of the blackbody. One can get a glimpse of this layer in the left image in Fig. 2. We therefore assume that the emissivity is 0.95 with uncertainty 0.025.

Figure 2. Blackbodies at Stokes Hill Wharf. Left: The blackbodies were mounted side-by-side on the pier. A provisional "sun screen" kept the blackbodies out of direct sunlight. Right: Crop from the IRCAM LW image of the two blackbodies. The temperatures were $T_{cold} = 34.8\,^{\circ}\mathrm{C}$ and $T_{hot} = 48.6\,^{\circ}\mathrm{C}$.

2.3 Camera

The camera that provided the image data to the analysis was FFI's IRCAM LW camera. Some relevant characteristics are shown in Tab. 1. The camera was located at a height above sea level of about 5 m on average, the tidal variations being about 1 m.

The calibration procedure for this camera – both non-uniformity correction (NUC) and data calibration – involved the use of two small "hand held" blackbody water vessels, also painted with the same Nextel Velvet

Table 1. Characteristics of the IRCAM LW camera.

Spectral range	$7.5 - 9.9\,\mu$m
Focal length	200 mm
Array size	640×512
Pixel pitch	$16\,\mu$m
Horizontal Field of View (FOV)	2.93°
Instantaneous FOV (IFOV)	$80\,\mu$rad

Coating 811-21 as the target blackbodies. The temperature of these calibration blackbodies were measured by a Fluke 572-2 IR thermometer (an "IR-pistol"), with an emissivity setting at $\epsilon = 0.95$. Our experience with thermometers of this kind informs us that the accuracy of the measured temperatures is about 1 °C.

2.4 Meteorology

FFI used two weather stations during the trial, which provide input to the analysis. One Vaisala WXT520 was mounted at the measurement site at East Arm Wharf, and another Vaisala WXT520 was mounted close to the target blackbodies at Stokes Hill Wharf. These weather stations provided measurements of air pressure, air temperature, relative humidity and (24h average) wind speeds.

In addition, a Biral VPF-730 visibility sensor (FFI) was also mounted at East Arm Wharf and used to measure optical range (2% visibility).

The precision of the various measured quantities from these sensors (which is needed for the sensitivity analysis) can be found from the manuals, with one notable exception. The air temperature T_{air} is measured by an instrument that was mounted on a pole and has a precision of 0.3 °C. However, this parameter is used for the temperature of the atmospheric path from detector to target over sea, and also for the camera temperature (in the calibration procedure, see Sec. 3.1). A more realistic uncertainty for T_{air} is 1 °C. Also, this is the same as the uncertainty in the blackbody temperatures, which allows us to compare effects.

The list of parameters and their uncertainties is shown in Sec. 5.2.

3. THE MODEL – EQUIVALENT BLACKBODY TEMPERATURE

IR signature analysis involves computing the equivalent blackbody temperature difference between the target and background. In order to achieve this, the equivalent temperature T_{eq} must be computed for each pixel in the IR image, i.e. for each detector element. This computation of T_{eq} is *the model* that we will subject to the sensitivity analysis in this paper.

3.1 T_{eq} theory

The theory behind the computation of T_{eq} has been described in Ref. 5. Let us repeat some relevant steps here.

The signal received at a detector element (pixel) from the target is given by

$$S_{tgt} \;=\; S_0 + K \int_0^\infty \left[N_{tgt}(\lambda)\tau_{atm}(\lambda, x) + N_{atm}(\lambda, x) \right] r_s(\lambda) d\lambda, \tag{1}$$

where

S_0	is the camera offset,
K	is the gain,
$N_{tgt}(\lambda)$	is the radiance from the target,
$N_{atm}(\lambda, x)$	is the radiance from the path between sensor and target,
$\tau_{atm}(\lambda, x)$	is the atmospheric transmittance,
$r_s(\lambda)$	is the relative spectral response of the detector,
λ	is wavelength, and
x	is the distance to the target.

Furthermore, the spectral radiance from the atmosphere, assuming a horizontal path with constant temperature, is

$$N_{atm}(\lambda, x) = (1 - \tau_{atm}(\lambda, x))\, N_{bb}(\lambda, T_{atm}), \tag{2}$$

where T_{atm} is the atmospheric temperature and $N_{bb}(\lambda, T)$ is the spectral radiance from a blackbody of temperature T:

$$N_{bb}(\lambda, T) = \frac{2c^2 h}{\lambda^5 \left(e^{hc/\lambda kT} - 1\right)}. \tag{3}$$

Here, c is the speed of light in vacuum, h is Planck's constant and k is Boltzmann's constant.

Our goal is to determine the equivalent temperature T_{eq} of a perfect blackbody (emissivity $\epsilon = 1$) at the location of the target so that we get the same signal at the detector. That is, if we replace $N_{tgt}(\lambda)$ with $N_{bb}(\lambda, T_{eq})$ in Eq. (1), we should get the same signal S_{tgt}.

The calculation of T_{eq} proceeds in a number of steps:

1. *Determine gain K and offset S_0.* This is a calibration step. The inputs are recordings of a cold and a hot blackbody (BB1 and BB2) held up in front of the camera lens, their temperatures T_1 and T_2, their emissivities $\epsilon_1 = \epsilon_2 = \epsilon$, the camera temperature T_{cam}, and the spectral relative response function $r_s(\lambda)$ for the camera system (detector + lens). The target radiance in this case is a sum of two terms:

$$N_{tgt}(\lambda) = \epsilon N_{bb}(\lambda, T_i) + (1 - \epsilon) N_{bb}(\lambda, T_{cam}), \qquad i = 1 \text{ or } 2, \tag{4}$$

   where the first term is the emitted blackbody radiance from BB1 or BB2 and the second term is the radiance from the camera (a blackbody at temperature T_{cam} and emissivity $\epsilon_{cam} = 1$) reflected from the surface of BB1 or BB2 (with reflectivity $\rho = 1 - \epsilon$).

   Assuming the atmospheric transmittance is close to 1 for the short path of atmosphere between the lens and the calibration blackbodies, we can use Eq. (1) to first find K from the expression

$$S_2 - S_1 = K\epsilon \int_0^\infty \left[N_{bb}(\lambda, T_2) - N_{bb}(\lambda, T_1)\right] r_s(\lambda) d\lambda, \tag{5}$$

   and then S_0 from

$$S_0 = S_1 - K \int_0^\infty \left[\epsilon N_{bb}(\lambda, T_1) + (1 - \epsilon) N_{bb}(\lambda, T_{cam})\right] r_s(\lambda) d\lambda. \tag{6}$$

2. *Calculate the atmospheric transmittance τ_{atm}.* MODTRAN is used to calculate the transmittance in the spectral range we are interested in (determined by $r_s(\lambda)$). A user-defined model of the atmosphere was used for this, with one layer where air pressure, air temperature, and relative humidity was specified. The spectral resolution was 1 cm^{-1}. Other input parameters were 2% visibility, 24h average wind, camera elevation and range to target. The C++ programming API for MODTRAN6[1] was used in actual computations for our analysis, but we have included an example of an input file in json-format in Appendix A, with typical parameters.

3. *Solve the equation for T_{eq} numerically.* Again using Eq. (1), the equation to solve is

$$\int_0^\infty N_{bb}(\lambda, T_{eq}) \tau_{atm}(\lambda, x) r_s(\lambda) d\lambda = \frac{S_{tgt} - S_0}{K} - \int_0^\infty N_{atm}(\lambda, x) r_s(\lambda) d\lambda. \tag{7}$$

   This is essentially a root finding problem, and can be solved for instance by using bisection.

3.2 Specifying the model

A model calculation may depend on a large number of parameters, so a part of the task is to determine which parameters are to be included in the model specification, and which parameters are left out. In our case, we have a model of the type $T_{eq} = f(X_1, X_2, \ldots, X_k)$, where $X_i, i = 1, \ldots, k$, are the k parameters. We have chosen a set of 10 parameters in total, which are typical parameters that are measured during a field trial and used in signature analysis. The parameters fall roughly into two groups:

- Calibration parameters: Blackbody temperatures T_1 and T_2, emissivity ϵ, and camera temperature T_{cam}. T_1 and T_2 were measured immediately after making calibration recordings, which were made either before or after each run during the trial. ϵ was not measured during the trial – the value that was discussed in Sec. 2.3 was used (0.95). There was no separate measurement of the camera temperature. However, the camera was located outdoors, so as an approximation the air temperature was used: $T_{cam} = T_{air}$.
- Parameters that are input to MODTRAN: Air pressure p, air temperature T_{air}, relative humidity rh, 2% visibility vis, 24 h average wind whh, camera elevation $h1$, and range to target r. These parameters were measured by our weather stations on site, as described in Sec. 2.4, except $h1$ and r which were fixed constant values.

(Since T_{air} was used for T_{cam}, T_{air} is in both groups.) From these parameters and their uncertainties, we are able to assess the contributions from calibration and MODTRAN simulations to the uncertainties in T_{eq} calculations.

3.3 What is not included in the model?

Numerous other parameters enter into the theory and contribute to the final result, but were considered to be "fixed" in the present context. Some of the more important ones are:

- The detector signal from the target pixel, S_{tgt}. In our analysis, we identified the hot pixel in an image from Stokes Hill Wharf, see Fig. 2, and used that as a fixed value in our calculations. In principle we could have included this value as a parameter in the sensitivity analysis, but this was considered outside the scope of the present analysis. Also, only a single pixel from a single image was used – no averaging over a region or over time. This would require more involved calculations with no new information. We checked that the value of the chosen pixel was representative (not an outlier) of the full time series of the recording. See also the discussion in Sec. 6.
- The signals recorded from the two calibration blackbodies, S_1 and S_2. The argument for not including them as parameters to the model is similar to the one for S_{tgt}. However, the values for S_1 and S_2 were obtained by averaging recordings of 100 images of each blackbody, which means that the precision of these values were much better than S_{tgt}.
- The relative spectral response of the camera system $r_s(\lambda)$. This response curve has been measured with special calibration equipment at FFI. Uncertainties in the measurement points on the curve are unknown, but based on our knowledge of this equipment, we assume these to be small.

It is of course important to realize that the model depends indirectly on these left-out parameters, and that output uncertainty as a function of input uncertainty depends on where these parameters have been fixed.

4. VARIANCE-BASED SENSITIVITY ANALYSIS

There are several methods to evaluate the effects of uncertainty in the input parameters on model output. See Refs. 2 and 6 for reviews.

Sensitivity analysis can be performed for a variety of reasons. One reason is to explore how good the model is to describe the physical system ("data modelling") in a variety of conditions. In that case the distribution functions that describe the input parameters should be different from those we use here, like for example uniformly

distributed in some admissible interval, or normally distributed with "large" standard deviations (larger than the measurement errors).

In this paper we are interested in how typical measurement errors in the input propagate to the model output. This means that our k input parameters are considered to be random variables, whose mean values are the measured values, and standard deviations are the estimated measurement uncertainties. We will use the variance-based sensitivity analysis that has been developed by Saltelli and others.[2,3] We give a brief description here for completeness. Readers may consult the references for more details.

4.1 Theoretical considerations

We are given a model of the type

$$Y = f(X_1, X_2, \ldots, X_k), \tag{8}$$

where Y, a scalar, is the output from the model, and $X_i, i = 1, \ldots k$, are input parameters. The input parameters are assumed to be distributed according to some probability distribution, e.g. uniformly on $[0, 1]$ or normally $X_i \sim \mathcal{N}(\bar{X}_i, \sigma_i)$. In a variance-based sensitivity analysis the goal is to compute two sets of "sensitivity indices": The *first order sensitivity index* of parameter i,

$$S_i = \frac{V_{X_i}(E_{\mathbf{X}_{\sim i}}(Y|X_i))}{V(Y)}, \tag{9}$$

and the *total effect index* of parameter i,

$$S_{Ti} = \frac{E_{\mathbf{X}_{\sim i}}(V_{X_i}(Y|\mathbf{X}_{\sim i}))}{V(Y)}. \tag{10}$$

In these expressions, $E(\cdot)$ is the expectation value and $V(\cdot)$ is the variance. $\mathbf{X}_{\sim i}$ denotes the set of all parameters *except* X_i. In plain words, the two indices have the following interpretation (referring to Eqs. (9) and (10)):

S_i: First fix X_i momentarily, find the expectation value of Y as all the other parameters are varied, take the variance of this over X_i, and finally normalize by dividing by the total variance.

S_{Ti}: First fix all parameters except X_i momentarily and find the variance of Y, take the expectation value of this as all these parameters are varied, and then normalize by dividing by the total variance.

What does this mean? Some comments may be helpful:[2,3]

- The S_i represent the *direct* contribution from X_i to the variance in Y. They are always numbers between 0 and 1.
- The S_{Ti} represent the contributions to the variance in Y coming from *all* effects involving X_i, including interaction effects with other parameters.
- S_i quantifies the expected reduction of variance that would be obtained if X_i could be fixed.
- S_{Ti} quantifies the expected variance that would be left if all parameters but X_i could be fixed.
- "Factor prioritization": A high value of S_i implies that X_i is "important" and that a reduction of the uncertainty of X_i will improve the accuracy of the model.
- "Factor fixing": A low value of S_{Ti} implies that the model is insensitive to errors in X_i, at least for the region of parameter space we are operating.

4.2 Estimators

In order to compute the sensitivity indices, a sampling-based scheme may be used. Several possible estimators have been developed, depending on details of the scheme. We have chosen to use the Monte Carlo sampling scheme that is recommended in Ref. 3, because it is straightforward to implement and has good convergence properties.

Let us assume for now that the X_i parameters that are arguments to the model function f are distributed uniformly on $[0, 1]$. We will discuss later how to handle normally distributed parameters.

First generate an $N \times 2k$ matrix of random numbers uniformly distributed on $[0, 1]$. N is a large number, say the order of a few thousands. Put the "left" part of this matrix into an $N \times k$ matrix $\mathbf{A}$ and the "right" part into an $N \times k$ matrix $\mathbf{B}$. Then define k matrices $\mathbf{A}_\mathbf{B}^{(i)}$ where all the columns of $\mathbf{A}_\mathbf{B}^{(i)}$ are from $\mathbf{A}$ except the i-th column which is from $\mathbf{B}$.

Each row in these matrices constitute k parameters, and is to be used as input to one run of the model. Run the model on the $N(2 + k)$ rows from the matrices $\mathbf{A}$, $\mathbf{B}$ and $\mathbf{A}_\mathbf{B}^{(i)}$ to produce the column vectors of results $f(\mathbf{A})_j$, $f(\mathbf{B})_j$ and $f(\mathbf{A}_\mathbf{B}^{(i)})_j, j = 1, \ldots, N$. The estimators are

$$S_i = \frac{1}{V(Y)} \cdot \frac{1}{N} \sum_{j=1}^{N} f(\mathbf{B})_j \left(f(\mathbf{A}_\mathbf{B}^{(i)})_j - f(\mathbf{A})_j \right) \tag{11}$$

and

$$S_{Ti} = \frac{1}{V(Y)} \cdot \frac{1}{2N} \sum_{j=1}^{N} \left(f(\mathbf{A})_j - f(\mathbf{A}_\mathbf{B}^{(i)})_j \right)^2, \tag{12}$$

where the estimators for mean and variance are

$$E(Y) = \frac{1}{N} \sum_{j=1}^{N} f(\mathbf{A})_j, \tag{13}$$

and

$$V(Y) = \frac{1}{N} \sum_{j=1}^{N} (f(\mathbf{A})_j)^2 - (E(Y))^2. \tag{14}$$

4.3 Quasi-random sequences

The matrix of $N \times 2k$ random numbers discussed above can be generated by a pseudo-random number generator. However, there is a problem with this, because the numbers that are generated on the interval $[0, 1]$ will have a certain "discrepancy", meaning that there may be gaps between the sample points. In general this leads to error terms in Monte Carlo integration – our case – that decreases as $1/\sqrt{N}$. In order to improve on this it is possible to use *quasi-random* number sequences, such as the Sobol sequence. See e.g. Ref. 7, ch. 7.7. The Sobol sequence is a low-discrepancy sequence, and leads to faster convergence. In general convergence is now of the order $1/N$.

It is recommended in Refs. 2 and 3 to use $2k$-dimensional Sobol sequences to generate the initial $N \times 2k$ matrix used in the sensitivity analysis. There is freely available code on the internet that generates uniformly distributed Sobol sequences on $[0, 1]$. We used the program `SOBOL_DATASET` from Ref. 8 for this task.

4.4 Conversion to normal distributions

We mentioned in Sec. 4.2 that we need to handle the conversion from uniform to normally distributed random numbers. We will consider the 10 parameters to our model for T_{eq} (described in Sec. 3) to be normally distributed numbers. That is, we consider these parameters to have a mean value equal to the measured values, and a standard deviation according to estimated uncertainties. The values we used are listed in Sec. 5.2.

The standard way to convert uniformly to normally distributed numbers is the Box–Muller method, see e.g. Ref. 7, ch. 7.2. This is easily applied to pairs of uniform parameters. One question that now arises is whether

the new set of converted, normally distributed, values has the correct low-discrepancy properties as the original Sobol sequence. That is, do the values of the distribution function as applied on the new sequence distribute uniformly on $[0, 1]$ with low discrepancy? In Ref. 9 it is shown that this is indeed the case.

Strictly speaking not all of the input parameters are normally distributed. For instance, relative humidity rh is a percentage, so it lies in the interval $[0, 100]$. A true normal distribution extends to $\pm\infty$. In order to get around this technicality, we assigned wide upper and lower bounds on all our parameters. For all practical purposes all the mean values were positioned far enough away from the bounds, measured in standard deviations, that they could be treated as normal for simplicity. Generated values were tested and re-drawn from a *pseudo-random* normal distribution if they happened to fall outside the admissible interval. This procedure might introduce a bias in the results, but the effect is very small.

5. SIMULATIONS AND RESULTS

5.1 Simulation setup

A C++ program was written to run the simulations and compute the sensitivity indices. A 20-dimensional Sobol sequence of N samples was generated using the program `SOBOL_DATASET`, as mentioned in Seq. 4.3. 20 dimensions corresponds to $2k$, where $k = 10$ is the number of parameters in our case. From this sequence the $2 + k$ matrices $\mathbf{A}$, $\mathbf{B}$ and $\mathbf{A}_{\mathbf{B}}^{(i)}$ were constructed.

We used different values for N in our simulations, with sample sizes of $N = 100, 500, 1000, 5000, 10000$. This allows us to check convergence of the computed sensitivity indices.

A Box–Muller transformation was applied on pairs of Sobol numbers to produce pairs of normally distributed numbers (mean 0, variance 1), and then transformed to get normally distributed numbers with the correct means and variances, see the next section. In this way each row of the matrices were transformed to a set of 10 input parameters to be used in model runs.

The parameter sets were then used to compute K and S_0, run MODTRAN, and estimate the indices. For the MODTRAN part we used batch running. The C++ API for MODTRAN6 provides the possibility to clone a "case" and use it as a template for other cases. Only parameters that are different from the template need to be specified.

The code was run on a Windows 10 workstation with an Intel Xeon Silver 4114 processor (2.2 GHz) and 32 GB of RAM. The case $N = 10000$ took about 95 minutes on this machine.

5.2 Parameter values and uncertainties

The list of parameters that were chosen to define the model was discussed in Sec. 3. The values to be used in the simulation were the ones measured at the time of the recording of the target blackbody at Stokes Hill Wharf. The precision of the parameters were discussed in Sec. 2. These are the standard deviations to be used for generating the distributions. Tab. 2 shows the list of parameters, the measured values, and estimated standard deviations.

5.3 Results

After running the simulations for $N = 10000$ we found the mean value and standard deviation of T_{eq} to be

$$T_{eq} = 43.6\,^{\circ}\mathrm{C}, \tag{15}$$

$$\sigma_{T_{eq}} = 2.9\,^{\circ}\mathrm{C}. \tag{16}$$

In comparison, a straightforward application of the model on the measured parameter values ("$N = 1$") yields

$$T_{eq} = 43.9\,^{\circ}\mathrm{C}. \tag{17}$$

The difference between Eqs. (15) and (17) is that Eq. (15) is an ensemble average, while Eq. (17) is not. The measured value of the target blackbody at Stokes Hill Wharf was

$$T_{tgt} = 48.6\,^{\circ}\mathrm{C}, \tag{18}$$

Table 2. Parameters of the model. The measured values and their standard deviations (uncertainties) are shown.

Parameter		Value	Std. dev.
T_1	BB1 temperature [°C]	29.2	1.0
T_2	BB2 temperature [°C]	39.3	1.0
ϵ	BB emissivity	0.95	0.025
T_{air}	Air temperature [°C]	28.7	1.0
p	Air pressure [mbar]	1005.6	1.0
rh	Relative humidity [%]	75	2
vis	2% visibility [km]	85	10
whh	Wind – 24 h average [m/s]	2.6	0.3
$h1$	Camera elevation [km]	0.005	0.001
r	Range to target [km]	3.4	0.01

which is much higher than the model value, to be discussed in Sec. 6.

The estimated values of the first order sensitivity indices S_i and total effect indices S_{Ti} are shown in Tab. 3. In order to get an idea about convergence, we have tabulated the the highest value for the two indices for

Table 3. Estimated first order sensitivity indices S_i and total effect indices S_{Ti}.

Parameter	S_i	S_{Ti}
T_1	0.5461	0.5469
T_2	0.1987	0.2077
ϵ	0.0238	0.0146
T_{air}	0.174	0.1836
p	0.0	0.0
rh	0.0578	0.0581
vis	0.0004	0.0001
whh	0.0	0.0
$h1$	0.0	0.0
r	0.0031	0.0002

different N in Tab. 4. Convergence is not perfect, but the numbers are sufficient to draw conclusions. We may

Table 4. Convergence. The values of S_{T_1} and S_{T,T_1} for increasing values of N.

Index	$N = 100$	$N = 500$	$N = 1000$	$N = 5000$	$N = 10000$
S_{T_1}	0.5233	0.5584	0.5033	0.5377	0.5461
S_{T,T_1}	0.4427	0.5493	0.526	0.5472	0.5469

also remark that preliminary simulations we have done using a standard *pseudo-random* number generator gave a much weaker convergence.

6. DISCUSSION

First of all, let us comment on the computed value $T_{eq} = 43.6\,°\mathrm{C}$ obtained from model calculations. It is lower than the measured value of the target. The difference is almost $2\,\sigma$, which appears to be large. The main reason for this discrepancy is of course due to the fact that the target is not a perfect blackbody. The target blackbody

had an emissivity of about $\epsilon = 0.95$. If we include this ϵ in the model calculation we find $T_{eq,\epsilon=0.95} = 47.1\,^{\circ}\mathrm{C}$, which is in fair agreement with the measured value $48.6\,^{\circ}\mathrm{C}$.

What about the remaining difference? There are several possible contributions to this:

- The target is small in terms of pixel extension – see Fig. 2, right image – just 1–2 pixels. A rigorous treatment would need to take the point spread function of the camera into account. A point source that is spread out in the image may lower the measured value at the centre.
- Pixel values may fluctuate because of noise in the detector system. Uncertainty from this was chosen not to be included in the model, as was discussed in Sec. 3.3.
- Fluctuations in the atmospheric conditions (turbulence).

Let us now turn to the main focus of this analysis – the sensitivity indices in Tab. 3. What do we learn from these numbers? The main lessons are:

- The total variance is dominated by the variance of three of the four parameters related to the calibration procedure: the calibration blackbody temperatures T_1 and T_2, and the air temperature T_{air}. This implies that the precision of equivalent temperature calculations is improved if these temperatures are measured more accurately.
- The cold calibration blackbody, BB1, is more important than the hot, BB2. This may seem unintuitive. The exact reason is not clear, but it may be related to the difference in radiances from the two blackbodies, and the fact that T_1 was closer to T_{air} in our case. It is *not* related to the unsymmetrical form of the equation for S_0, Eq. (6). We have tried a symmetrised form of this equation, involving both T_1 and T_2, but the result is the same.
- The variance of the other parameters, related to the MODTRAN part of the model, appear to have less impact on output variance – with T_{air} as an exception. This indicates that the model can be simplified by fixing some of the parameters (like camera elevation $h1$) on "typical" values, at least for a region of the parameter space.

  Note that contributions from the atmosphere are still important, even though the *uncertainties* in the meteorological parameters are not. Numerical experiments by varying the range to target can easily be performed to confirm this.
- The values of S_i and S_{Ti} are almost the same for each parameter. Since the difference between them is interaction effects, we find that the parameters are mainly uncorrelated in our model.

It would be interesting to try a similar sensitivity analysis of the same model to explore other parts of the parameters space, e.g. when other calibration data are recorded, or when the meteorological conditions are different. It would also be interesting to try to simplify the model by fixing the least significant MODTRAN parameters and then re-run the analysis.

In light of this analysis, we will investigate our calibration procedure further and test the sensitivity to T_1, T_2 and T_{air} for other cases, and also look into practical procedures to improve the precision of these measurements in field trials.

APPENDIX A. MODTRAN6 INPUT

MODTRAN was run from a C++ program in our analysis, using the new C++ API provided with MODTRAN6.[1] The input parameters were then specified in the C++ code. As an example, an equivalent specification of the parameters is given by the following file in json-format, with typical values of the parameters.

```
{
  "MODTRAN": [
    {
      "MODTRANINPUT": {
        "RTOPTIONS": {
          "IEMSCT": "RT_TRANSMITTANCE"
        },
        "ATMOSPHERE": {
          "MODEL": "ATM_CONSTANT",
          "M1": "ATM_CONSTANT",
          "M2": "ATM_CONSTANT",
          "M3": "ATM_CONSTANT",
          "M4": "ATM_CONSTANT",
          "M5": "ATM_CONSTANT",
          "M6": "ATM_CONSTANT",
          "MDEF": 1,
          "NPROF": 3,
          "NLAYERS": 1,
          "PROFILES": [
            {
              "TYPE": "PROF_PRESSURE",
              "UNITS": "UNT_PMILLIBAR",
              "PROFILE": [ 1005.6]
            },
            {
              "TYPE": "PROF_TEMPERATURE",
              "UNITS": "UNT_TCELSIUS",
              "PROFILE": [ 28.7]
            },
            {
              "TYPE": "PROF_H2O",
              "UNITS": "UNT_REL_HUMIDITY",
              "PROFILE": [ 75.0]
            }
          ]
        },
        "AEROSOLS": {
          "IHAZE": "AER_MARITIME_NAVY",
          "VIS": 85.0,
          "WHH": 2.6
        },
        "GEOMETRY": {
          "ITYPE": 1,
          "H1ALT": 0.005,
          "OBSZEN": 90.0,
          "HRANGE": 3.4
        },
        "SPECTRAL": {
          "V1": 1011.0,
          "V2": 1333.0,
          "DV": 1.0,
          "FWHM": 2.0,
          "FLAGS": "WTA    "
        },
        "FILEOPTIONS": {
          "NOPRNT": 2
        }

      }
    }
  ]
}
```


ACKNOWLEDGMENTS

We thank Lars Trygve Heen and Eirik Glimsdal for reading and commenting on the manuscript.

REFERENCES

[1] A. Berk, P. Conforti, R. Kennett, T. Perkins, F. Hawes, and J. van den Bosch, "MODTRAN6: a major upgrade of the MODTRAN radiative transfer code," in *Algorithms and Technologies for Multispectral, Hyperspectral, and Ultraspectral Imagery XX*, *Proc. SPIE* **9088**, p. 90880H, 2014.

[2] A. Saltelli, M. Ratto, T. Andres, F. Campolongo, J. Cariboni, D. Gatelli, M. Saisana, and S. Tarantola, *Global Sensitivity Analysis. The Primer*, John Wiley & Sons, 2008.

[3] A. Saltelli, P. Annoni, I. Azzini, F. Campolongo, M. Ratto, and S. Tarantola, "Variance based sensitivity analysis of model output. Design and estimator for the total sensitivity index," *Computer Physics Communications* **181**, pp. 259–270, 2010.

[4] E. T. Kwor and S. Matteï, "Emissivity measurements for Nextel Velvet Coating 811-21 between −36 °C and 82 °C," *High Temperatures – High Pressures* **33**, pp. 551–556, 2001.

[5] E. Stark, L. T. Heen, and K. Wikan, "SIMVEX 2001 trial – radiant intensity contrast," Tech. Rep. FFI/RAPPORT-2002/02568, FFI, 2002.

[6] J. C. Helton, J. D. Johnson, C. J. Sallaberry, and C. B. Storlie, "Survey of sampling-based methods for uncertainty and sensitivity analysis," *Reliability Engineering and System Safety* **91**, pp. 1175–1209, 2006.

[7] W. H. Press, S. A. Teukolsky, W. T. Vetterling, and B. P. Flannery, *Numerical Recipes in FORTRAN: The Art of Scientific Computing*. Cambridge University Press, second ed., 1992.

[8] J. Burkardt, "SOBOL_DATASET – Generate Sobol Datasets." Code for C++/Fortran 90/Matlab/Python, https://people.sc.fsu.edu/~jburkardt/cpp_src/sobol_dataset/sobol_dataset.html. License: GNU LGPL. (Accessed: 17 July 2018).

[9] G. Ökten and A. Göncü, "Generating low-discrepancy sequences from the normal distribution: Box–Muller or inverse transform?," *Mathematical and Computer Modelling* **53**, pp. 1268–1281, 2011.